



# I-124 PET/CT image-based dosimetry in patients with differentiated thyroid cancer treated with I-131: correlation of patient-specific lesional dosimetry to treatment response

Donika Plyku<sup>1,2,3,5</sup> · Robert F. Hobbs<sup>3,4</sup> · Di Wu<sup>1,2</sup> · Carlos Garcia<sup>2</sup> · George Sgouros<sup>3,4</sup> · Douglas Van Nostrand<sup>1,2,5</sup>

Received: 5 April 2021 / Accepted: 12 July 2021 / Published online: 4 February 2022  
© The Author(s) under exclusive licence to The Japanese Society of Nuclear Medicine 2022

## Abstract

**Purpose** The objective of this study is to evaluate the lesion absorbed dose (AD), biological effective dose (BED), and equivalent uniform dose (EUD) to clinical–response relationship in lesional dosimetry for <sup>131</sup>I therapy.

**Methods** Nineteen lesions in four patients with metastatic differentiated thyroid cancer (DTC) were evaluated. The patients underwent PET/CT imaging at 2 h, 24 h, 48 h, 72 h, and 96 h post administration of ~33–65 MBq (0.89–1.76 mCi) of <sup>124</sup>I before undergoing <sup>131</sup>I therapy. The <sup>124</sup>I PET/CT images were used to perform dosimetry calculations for <sup>131</sup>I therapy. Lesion dose–rate values were calculated using the time–activity data and integrated over the measured time points to obtain AD and BED. The Geant4 toolkit was used to run Monte Carlo on spheres the same size as the lesions to estimate EUD. The lesion AD, BED, and EUD values were correlated with response data (i.e. change in lesion size pre- and post-therapy): complete response (CR, i.e. disappearance of the lesion), partial response (PR, i.e. any decrease in lesion length), stable disease (SD, i.e., no change in length), and progressive disease (PD, i.e., any increase in length).

**Results** The lesion responses were CR and PR (58%, 11/19 lesions), SD (21%, 4/19), and PD (21%, 4/19). For CR and PR lesions, the ADs, BEDs and EUDs were > 75 Gy for 82% (9/11) and < 75 Gy for 18% (2/11). The ADs and BEDs were < 75 Gy for SD and PD lesions.

**Conclusion** By performing retrospective dosimetry calculations for <sup>131</sup>I therapy based on <sup>124</sup>I PET/CT imaging, we evaluated the correlation of three dosimetric quantities to lesional response. When lesion AD, BED, and EUD values were > 75 Gy, 47% (9/19) of the lesions had a CR or PR. The AD, BED, and EUD values for SD and PD lesions were < 75 Gy. The data presented herein suggest that the greater the lesion AD, BED, and/or EUD, the higher the probability of a therapeutic response to <sup>131</sup>I therapy.

**Keywords** Dosimetry · Imaging · Differentiated thyroid cancer · Radionuclide therapy · Response

Donika Plyku and Robert F. Hobbs are co-first authors.

✉ George Sgouros  
gsgouros@gmail.com

✉ Douglas Van Nostrand  
douglas.van.nostrand@medstar.net

Donika Plyku  
donika.plyku@medstar.net

<sup>1</sup> Division, Nuclear Medicine Research, MedStar Health Research Institute, Hyattsville, MD, USA

<sup>2</sup> Division of Nuclear Medicine, MedStar Washington Hospital Center, Washington, DC, USA

<sup>3</sup> Radiological Physics Division Department of Radiology and Radiological Sciences, Johns Hopkins University, School of Medicine, 1550 Orleans St., CRBII 4M.61, Baltimore, MD 21231, USA

<sup>4</sup> Department of Radiation Oncology and Department of Radiology and Radiological Sciences, Johns Hopkins University, School of Medicine, 1550 Orleans St., CRBII 4M.62, Baltimore, MD 21231, USA

<sup>5</sup> Nuclear Medicine Research, Georgetown University School of Medicine, MedStar Health Research Institute and Washington Hospital Center, 110 Irving Street, N.W., Suite GA60F, Washington, DC 20010, USA

## Introduction

The determination of the optimal amount of the prescribed activity for  $^{131}\text{I}$  treatment of locoregional or distant metastases of differentiated thyroid cancer remains controversial, and two approaches exist [1, 2]: empirically determined fixed activity or a prescribed activity based on patient-specific dosimetry. The empiric fixed activities for the treatment of distant metastases have a wide range: 3.7–11.1 GBq (100–300 mCi) [3]. The dosimetric approach can be further divided into three groups: (i) the blood (as a surrogate for bone marrow) introduced by Benua et al. [4] and subsequently refined by others [5, 6]; (ii) the lesional dosimetry approach, such as by Thomas et al. [7] and (iii) a combination of the two. In regard to blood dosimetry, Benua [8] developed a protocol to limit the prescribed therapeutic activity of  $^{131}\text{I}$  to an activity that delivers no more than 2 Gy to the blood with additional recommendations when diffuse lung metastases were present. Thomas et al. [7] calculated the absorbed dose delivered to the lesions. The Medical Internal Radiation Dosimetry (MIRD) Committee methodology [5] calculated the absorbed dose to the bone marrow itself rather than to the whole blood compartment and selected upper limits to be 3 Gy (300 rad) and 30 Gy (3000 rad), to the bone marrow and lungs, respectively.

Generally, a fixed  $^{131}\text{I}$  activity is administered on the basis of disease characteristics and patient age, with the risk of under- or overtreatment [9]. On the other hand, superiority of one dosimetric method versus another can be evaluated if the specific method can be correlated with the treatment outcome (i.e., patient's response to therapy) provided that the dosimetry methodology used is sufficiently accurate and a favorable absorbed dose–response relationship is established. When used prospectively, the dosimetry approach can enable treatment optimization by maximizing the amount of activity administered to the patient within the constraints of toxicity [10], and when performed retrospectively can allow for the evaluation of tumor dose–response relationships [11–14]. Absorbed dose to target organs and lesions can be obtained following the classic MIRD absorbed fraction methodology using established phantom models [15] or a personalized dosimetry approach (e.g., patient-specific three-dimensional radiobiological dosimetry 3D-RD [16]). The calculated absorbed dose (AD) for  $^{131}\text{I}$  therapeutic activity amounts can then be correlated with lesion response using the clinical information acquired before and after therapy. Radiobiological dosimetry quantities that account for dose-rate variability and non-uniformity of intra-tumoral dose distribution, such as the biological effective dose (BED), and the equivalent uniform dose (EUD), can also be calculated and correlated with response.

Studies correlating dosimetrically determined  $^{131}\text{I}$  prescribed activity to treatment outcomes for DTC are very limited [10, 12–14]. Jentzen et al. [13] assessed the therapy response above the accepted AD thresholds of lesions and to explore the relationship between therapy response and minimum absorbed dose of small lesions, while Weirts et al. [13] assessed the dose–response relationship in a fixed therapeutic  $^{131}\text{I}$  activity approach using pre-therapeutic  $^{124}\text{I}$  PET/CT lesional dosimetry in a large group of patients. In addition, lesion AD, BED and EUD were assessed by Hobbs et al. in one pediatric patient dosimetry study [10]. The objective of this study is to evaluate the relationship between the lesional AD, BED, and EUD to clinical response in lesional dosimetry for  $^{131}\text{I}$  therapy performed based on  $^{124}\text{I}$  PET/CT imaging.

## Materials and methods

### Patient selection and study overview

Nineteen lesions in four patients diagnosed with metastatic DTC at MedStar Health Washington Hospital Center (MWHC) and referred for  $^{131}\text{I}$  dosimetry are evaluated in this study. Patients were selected from a previously described prospective study [17]. All patients underwent  $^{124}\text{I}$  PET/CT imaging over four consecutive days before undergoing  $^{131}\text{I}$  therapy. In this study we performed patient and lesion-specific dosimetry calculations for  $^{131}\text{I}$  therapy based on the  $^{124}\text{I}$  PET/CT imaging data.

### Patient preparation, $^{124}\text{I}$ PET/CT imaging, and $^{131}\text{I}$ therapy

Patient preparation has been discussed elsewhere [17]. Patient preparation for  $^{124}\text{I}$  PET/CT imaging and  $^{131}\text{I}$  therapy was done using either intramuscular injections of recombinant human thyroid stimulating hormone (rhTSH) on two consecutive days or thyroid hormone withdrawal (THW) for 4 weeks, Table 1. Specifically, for the latter, the patients discontinued taking thyroxine and began liothyronine sodium (Cytomel®; Pfizer) (25 mg 2–3 times/day for 21 days). After preparation with either rhTSH or THW, the patients were administered 33–65 MBq (0.80–1.76 mCi) of  $^{124}\text{I}$  orally, Table 1. PET/CT imaging was performed at 2 h, 24 h, 48 h, 72 h and 96 h post-administration of  $^{124}\text{I}$ . The patients were imaged using a Philips Gemini TF (Time-of-Flight) PET/CT camera. Depending upon the acquisition time post administration, imaging duration was 2- or 4 min/bed position and 16 bed positions were acquired for the whole body. The PET images are reconstructed following standard PET reconstruction techniques as implemented in the Philips Gemini ToF camera system. The CT attenuation scans are acquired

**Table 1**  $^{124}\text{I}$  diagnostic and  $^{131}\text{I}$  therapeutic administered activities

	Patient preparation method for $^{124}\text{I}$ PET/CT imaging and $^{131}\text{I}$ therapy	$^{124}\text{I}$ Activity MBq (mCi)	$^{131}\text{I}$ Activity MBq (mCi)
Pt1	THW	29 (0.78)	11,803 (319)
Pt2	THW	65 (1.76)	14,726 (398)
Pt3	THW	36 (0.98)	7,326 (198)
Pt4	rhTSH	33 (0.89)	6,623 (179)

using 120 keV and 30 mAs; and PET reconstruction is performed using ordered subset expectation maximization-TF (OSEM-TF) reconstruction with segmented attenuation correction using the CT data. The sensitivity of the camera was measured by imaging an  $^{124}\text{I}$  standard of a known activity.

All patients underwent  $^{131}\text{I}$  therapy after being prepared with rhTSH or THW, depending on the preparation method used for  $^{124}\text{I}$  PET/CT imaging, Table 1. The  $^{124}\text{I}$  PET/CT imaging time points were used to calculate AD, BED, and EUD of the 19 lesions as described below. These calculations were not used in the determination of the administered activity of the therapeutic  $^{131}\text{I}$  that the patients received during treatment.

### Dosimetry calculations for tumors

Tumor dosimetry calculations were performed using a hybrid methodology, where the tumor self-dose rate for each time point,  $t$ , was obtained using the MIRD formalism (MIRD Pamphlet 21) [18], according to the formula:

$$\dot{D}_{\text{self}}(t, \text{tumor}) = A(t, \text{tumor}) \cdot S(\text{tumor} \leftarrow \text{tumor}), \quad (1)$$

where  $A$  is the activity at time point  $t$ , and  $S$  is the  $S$  value, assumed to be time-independent. The external photon contribution from the remainder of the body to the lesion was done by measuring the photon contribution of  $^{131}\text{I}$  from the whole body to a nearby region of background uptake using Monte Carlo simulation of the registered images.

The tumor time–activity data were obtained following a previously described quantitative method that corrects for background and partial volume effects in PET [17, 19]. Tumor contours were drawn using the imaging software Velocity® with guidance from a nuclear medicine physician to delineate the lesion on the CT image. The four subsequent PET/CT images are co-registered to the first time-point CT image using a deformable registration algorithm available in Velocity software. Tumor contours were drawn both on the first time-point CT image as well as on each individual time-point PET image. The registration across different time-points facilitates superimposing the CT-drawn tumor volume with the volumes drawn on the PET images for the same tumor and partially account for the different positions of the tumors across time-points. The

CT-defined volume was considered as the “real” volume of the tumor. To account for spill-out, the tumor activity volumes were drawn using a minimum threshold of the maximum PET value on each PET image. Figure 1a–d shows examples of tumor contours drawn on the PET images for Pt1 (a–b) and Pt3 (c–d). The lesion activity was calculated by considering the different activity contributions to the threshold-based volumes and the CT-defined volume. The background activity concentration was also measured by drawing contours on the PET images at specific locations on the patient’s body (i.e., bone, bone marrow and lungs) according to tumor locations and then multiplying with the threshold-based contour volume ( $\text{cm}^3$ ) to obtain total background activity in counts. Subsequently, this quantity was subtracted from the threshold-based volume activity for the difference of the PET-based and CT-based volumes, i.e.: the background activity in the larger spill-out region was not added to the lesion activity, only the excess spill-out activity was added back to the lesion activity. The resulting estimate of tumor activity at each time-point was used to generate time–activity curves for each lesion. Examples of time–activity curves for a CR, PR, SD and PD tumor are given in Fig. 2. All lesional time–activity data displayed an uptake phase from the initial time-point (2 h) up to the 2nd or 3rd time-point (24 h or 48 h) and a clearance phase beyond 24 h or 48 h up to the last measured time-point (96 h). The data were fit with hybrid trapezoid-exponential functions and integrated to obtain the time-integrated activity.

The  $S$  values were obtained by fitting the  $S$  values from  $^{131}\text{I}$  OLINDA/EXM sphere model to a power law formula:

$$S = a \cdot m^b \quad (2)$$

where  $m$  is the tumor mass in gram (g). The values for the parameters were  $a = 108 \text{ mGy/MBq-hr-g}$  and  $b = -0.97$  which were then used for each tumor using the tumor mass.

The dose rate contribution from the whole body was obtained using 3D RD. The images were registered across time and a surrogate region of interest (ROI) in a proximal normal organ with low uptake was chosen for each tumor. Monte Carlo of the photon component only was simulated for each time-point and the energy collected in the ROI and divided by mass to obtain a dose rate for each

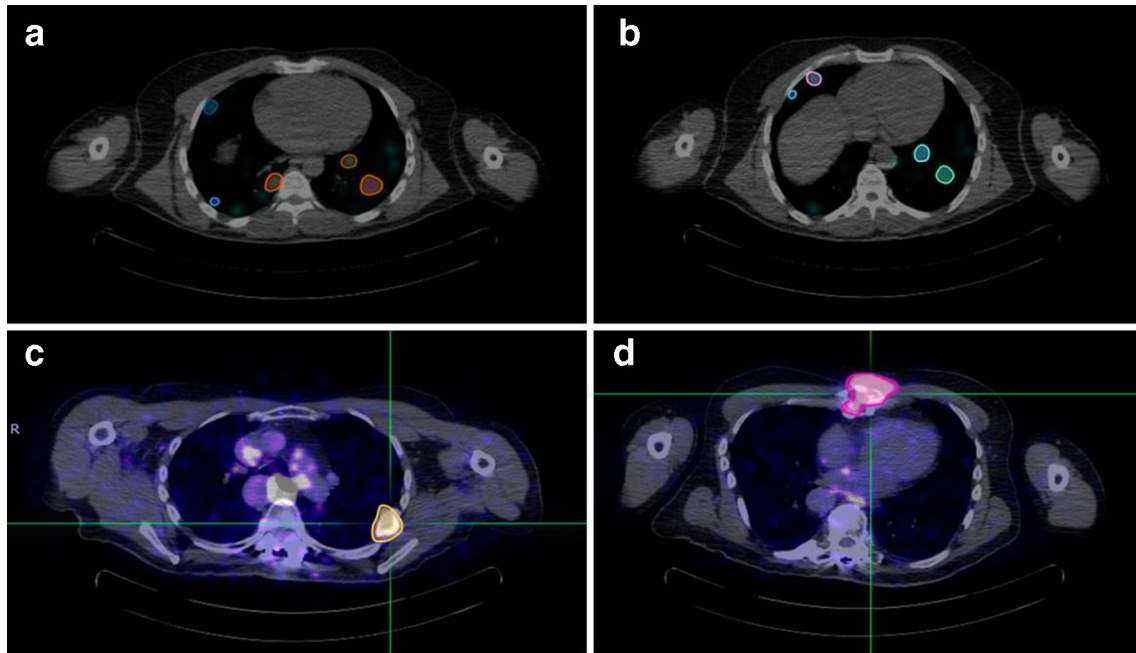


**Fig. 1** Examples of tumor contours drawn on the PET images for Pt1–48 h PET image (a), Pt3–72 h PET image (b), Pt3–tumor#2 (c), and Pt3–tumor#5 (d)

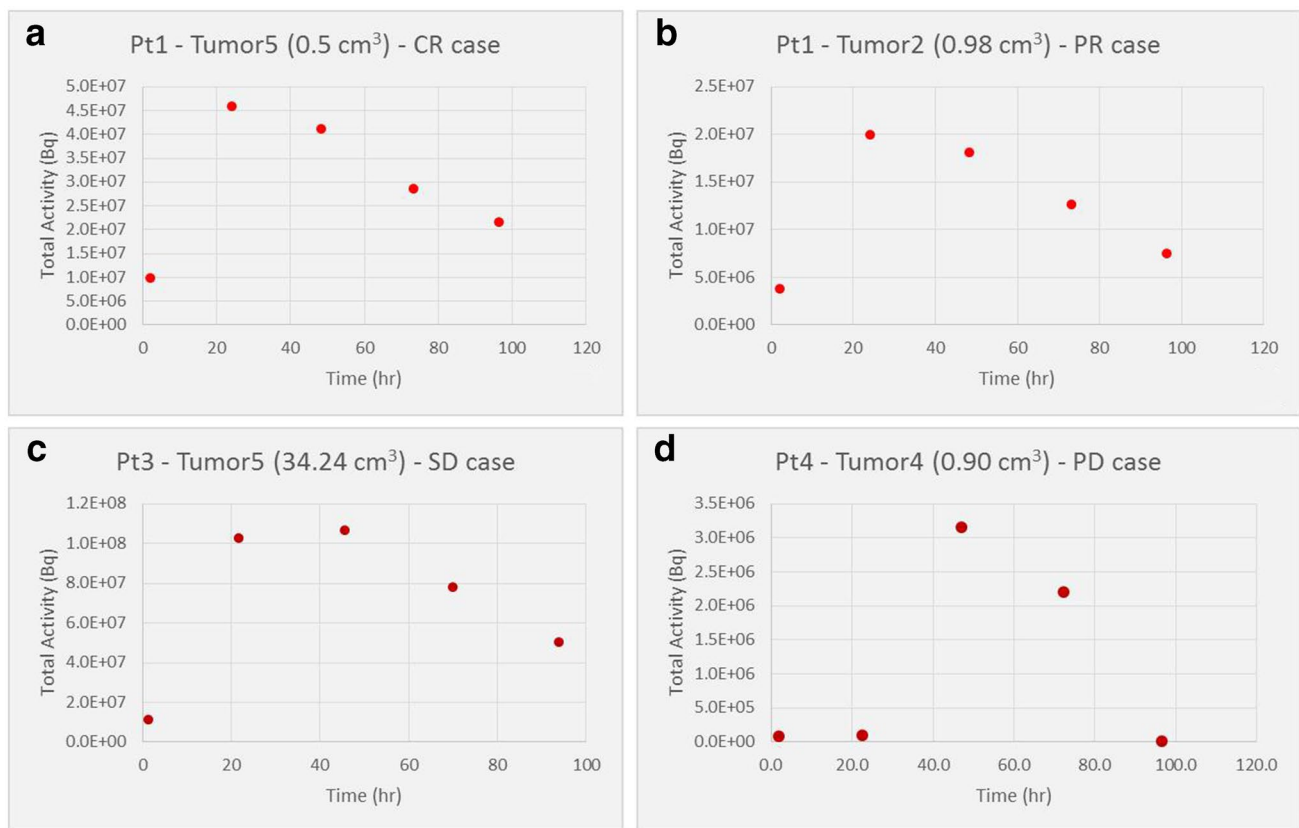


**Fig. 2** Examples of time–activity graphs for four tumor cases: CR (a), PR (b), SD (c) and PD (d)



time-point. These values were used as cross-dose rates for the tumor. The cross-dose-rate values were then added to the tumor self-dose-rate to obtain tumor total dose-rate for each PET time-point. The total dose-rate data were plotted versus the measured time-points and integrated to obtain tumor absorbed dose. This integration was done using a hybrid (trapezoidal + exponential) fit, trapezoidal integration from 0 to 24 h or 48 h, and exponential fit beyond 24 h or 48 h to infinity.

### Calculation of lesion biological effective dose (BED)

The BED was calculated as implemented in 3D-RD patient-specific dosimetry software [10, 16, 20–22]. The BED has been defined as [23, 24]:

$$\text{BED} = D \left( 1 + \frac{G(\infty)}{\alpha/\beta} \cdot D \right) \quad (3)$$

where  $\alpha$  and  $\beta$  are the linear-quadratic radiobiological parameters [25],  $D$  is the absorbed dose, and  $G(t)$  is the Lea-Catcheside factor [26, 27].  $G(T)$  is given as:

$$G(T) = \frac{2}{D^2} \cdot \int_0^T D(t) dt \int_0^t D(w) \cdot e^{-\mu(t-w)} dw \quad (4)$$

where  $w$  and  $t$  are integration variables,  $\mu$  is the repair rate for DNA damage assuming exponential repair. For a piecewise defined function and analytical formula cannot be established for the BED as it is time-dependent and depends on the full knowledge of the dose-rate function from time 0 to the desired time-point; however, the BED can be calculated numerically [20, 21]. First, the  $G(T)$  factor for each lesion was calculated in 3D RD. Then, the calculated AD values and  $G(T)$  per lesion were used in Eq. 3 to obtain lesion BED. The radiobiological parameters ( $\alpha$ ,  $\beta$  and  $\mu$ ) depend on many clinical and methodological factors and the selection of accurate values for  $\alpha$ ,  $\beta$  and  $\alpha/\beta$  ratio is pivotal for a reliable estimate of radiation response [28]. These parameters should be selected based on tumor site, histology and the applied linear quadratic model [28]:  $\alpha$  and  $\beta$ , represent the intrinsic radio-sensitivity of the irradiated cells (i.e. cells with a higher  $\alpha$  and  $\beta$  are more sensitive to radiation). The ratio of the two parameters,  $\alpha/\beta$ , is a measure of the fractionation sensitivity of the cells: cells with a higher  $\alpha/\beta$  are less sensitive to the sparing effect of fractionation [28].

For a thyroid cancer-originated tumor, these values have been determined as:  $\alpha = 0.365 \text{ Gy}^{-1}$  and  $\beta = 0.028 \text{ Gy}^{-2}$  [16, 29, 30]. Therefore, the  $\alpha/\beta$  ratio used for the BED calculation in this study was  $\sim 13.04 \text{ Gy}$ . The repair rate ( $\mu$ ) was taken to be 1.3 [16, 31].

### Calculation of lesion equivalent uniform dose (EUD)

The EUD is a radiobiological derived dosimetric parameter intended to reflect the impact of non-uniform tumor absorbed dose (or BED) distributions on tumor control, accounting for the spatial non-uniformity of the relevant dosimetry quantity [32]. Radiobiological modeling was introduced by incorporating models derived from the linear quadratic equation [32]. The BED accounts for differences in dose-rate and the EUD accounts for the impact of spatial distribution on response. These models are implemented in 3D-RD by calculating absorbed dose rate images for each time-point rather than the integrated absorbed dose from the time-integrated activity map [32].

Using the dose-rate data,  $G(T)$  factors, and BED values calculated for each lesion as described above, we performed Monte Carlo simulations for spheres the size of the tumors to obtain EUD for a specific sphere mass/volume, assuming uniform activity distribution. The Geant4 toolkit [33] developed for nuclear physics research was utilized for this Monte Carlo simulation. The uniform activity simulations result in non-uniform dose distribution with a decreasing dose towards the edge of the tumors. This edge effect is a real consequence of energy deposition as opposed to the artificial edge effect from misallocation of activity from the partial volume effect. The energy was binned as a function of radial distance from the center of the sphere and the dose for each bin calculated. The BED for each bin was calculated using the same G-factor as for the entire tumor, i.e.: pharmacokinetics were assumed to be uniform for the entire tumor. The EUD for the tumor/sphere was then calculated by summing the bin BED values ( $\text{BED}_i$ ) weighted by bin mass ( $m_i$ ) using the following formula:

$$\text{EUD} = -\frac{1}{\alpha} \ln \left( \frac{\sum_{i=1}^N m_i e^{-\alpha \text{BED}_i}}{\sum_{i=1}^N m_i} \right) \quad (5)$$

where  $m$  is the mass of tumor  $i$  and BED is the calculated BED for tumor  $i$ ,  $\alpha$  is the radiobiological parameter – radio-sensitivity per unit dose (1/Gy).

### Pre-therapy and follow-up clinical evaluations

The pre-therapy lesion length measurements were performed using information from either the CT scan of the  $^{124}\text{I}$  PET/CT or the  $^{18}\text{F}$ -FDG PET/CT. The CT scan was an attenuation CT for the  $^{124}\text{I}$  PET/CT or either a diagnostic or an attenuation CT for the  $^{18}\text{F}$ -FDG PET/CT. After  $^{131}\text{I}$  therapy, lesion length measurements were performed using either a follow-up chest CT w/ contrast or the CT of the follow-up  $^{18}\text{F}$ -FDG PET/CT scan. Pre-therapy and follow-up scans were evaluated according to a modified Response Evaluation Criteria in Solid Tumors (RECIST).

According to RECIST 1.1 [34, 35], the target lesions (TL) are categorized as: complete response (CR: disappearance of all TL), partial response (PR: at least 30% decrease in sum of the diameters of TL using the baseline sum of the diameters of TL), progressive disease (PD: at least 20% increase in the sum of the diameters of TL taking as reference the smallest sum of the diameters of TL recorded since treatment started and also appearance of one or more new TLs) or stable disease (SD: neither sufficient shrinkage to qualify for PR, nor sufficient increase to qualify for PD). The modification of the RECIST 1.1 criteria for this study consisted of the following: CR if the lesion was not visualized on the follow-up scan; PR if the lesion had any decrease in length or longest diameter, SD if the lesion had no change in length, and PD if lesion had an increase in length. This modification was adopted because the majority of the lesions were pulmonary metastases and typically smaller than the 1 cm measurement that is required by the RECIST criteria. PET response criteria in solid tumors (PERCIST) were not performed for response evaluation.

The original prospective study forming the source of this analysis of the data presented herein as well as this study itself was approved by the MedStar Health

Institutional Review Board, and all patients signed a written informed consent.

## Results

A total of 19 lesions/tumors were identified: 9, 2, 4, and 4 lesions in these four patients, respectively. Patients' ages were 47, 30, 63 and 62 years old. Patients are labeled as Pt1-Pt4. The  $^{124}\text{I}$  administered activity for each study and the administered activity for  $^{131}\text{I}$  therapy are listed in Table 1. Histology type, localization of lesions, lesion diameter/length changes before and after therapy are given in Table 2. Lesion length decreased for Pt1 in the follow-up scans for all lesions, which were labeled as PR or CR (lesion no longer seen on the follow-up scan). The CT images for Pt2 (2 lesions) acquired before and after therapy demonstrated a decrease in length for one lesion and no change for the 2nd lesion. Pt3 follow-up scans showed a decrease in lesion size for one lesion and no change for the remaining lesions. Lastly, Pt4 exhibited an increase in length for all lesions on the follow-up scan compared to the pre-therapy scans.

Patients 1–3 had a successful and/or stable response to therapy—complete response (CR), partial response (PR)

**Table 2** Lesion length change pre- and post-therapy

Patient	Histology type	Localization of metastases	Tumor # and response label	Pre-therapy lesion length <sup>a</sup> (mm)	Post-therapy lesion length <sup>b</sup> (mm)	Change in lesion length post-therapy
Pt1	FTC	Pulmonary	1-PR	5.0	4.2	− 0.8
			2-PR	5.4	5	− 0.4
			3-PR	5.9	5.2	− 0.7
			4-PR	5.0	3.5	− 1.5
			5-CR	4.6	0	− 4.6
			6-CR	9.6	0	− 9.6
			7-CR	5.9	0	− 5.9
			8-PR	5.7	5.5	− 0.2
			9-CR	3.2	0	− 3.2
Pt2	PTC	Pulmonary	1-PR	6.3	5.6	− 0.7
			2-SD	5.0	5.0	0
Pt3	FTC	Bone and bone marrow	1-SD	3.0	3.0	0
			2-PR	4.0	3.3	− 0.7
			3-SD	3.0	3.0	0
			4-SD	5.0	5.0	0
Pt4	PTC	Pulmonary	1-PD	18	37	+19
			2-PD	6.2	13	+6.8
			3-PD	10.8	18.5	+7.7
			4-PD	6.5	9.3	+2.8

FTC follicular thyroid carcinoma, PTC papillary thyroid carcinoma)

<sup>a</sup>The pre-therapy lesion length measurements were performed using information from either the CT scan of the  $^{124}\text{I}$  PET/CT or the  $^{18}\text{F}$ -FDG PET/CT

<sup>b</sup>After  $^{131}\text{I}$  therapy, lesion length measurements were performed using either a follow-up chest CT w/ contrast or the CT of the follow-up  $^{18}\text{F}$ -FDG PET/CT scan

and/or stable disease (SD), while Pt4 had 100% progressive disease (PD). The total response rate (CR, PR) in 4 patients (19 lesions) was 58% (11/19 lesions). The lesion volumes as determined by the CT-drawn VOI in four patients ranged from 0.06 to 46.9 ml. A total of 95 contours were drawn for the 5 PET/CT time-points and 19 lesions. The AD delivered to the lesions determined to be CR and PR ranged from 18.3 to 953.4 Gy, and the AD that the SD lesions received ranged from 3.3 to 33.8 Gy. AD values for Pt4 lesions (progressive disease patient) ranged from 11.1 to 71.6 Gy.

The AD per unit administered activity (AA) of <sup>131</sup>I and the calculated lesion AD, BED and EUD values are given in Table 3. Figures 3, 4 and 5 show the calculated AD, BED and EUD per lesion versus lesional response, respectively.

Of those CR and PR lesions, the ADs, BEDs and EUDs were > 75 Gy for 82% (9/11) and < 75 Gy for 18% (2/11) of lesions. Of those SD and PD lesions, the ADs, BEDs and EUDs were < 75 Gy for all eight lesions.

### Discussion

This study is significant for four reasons.

First, this is the largest study to date comparing CT-based responses of distant metastases of DTC (e.g., primarily pulmonary) to absorbed dose, biological effective dose

**Table 3** Calculated tumor absorbed dose per unit administered activity (AD/AA) of <sup>131</sup>I and total absorbed dose, biological effective dose and equivalent uniform dose per lesion

Tumor #	Lesional response label	AD/AA (mGy/MBq)	AD (Gy)	BED (Gy)	EUD (Gy)
1	PR	7.3	86.3	119.3	78.0
2	PR	16.7	197.2	400.5	204.0
3	PR	20.8	244.9	488.0	248.0
4	PR	16.2	190.6	380.4	199.0
5	CR	80.8	953.4	3923.6	1710.0
6	CR	24.8	292.7	402.6	236.0
7	CR	41.3	486.8	767.6	427.0
8	PR	11.1	131.0	156.0	103.0
9	CR	16.4	193.9	374.0	194.0
1	PR	1.2	18.3	20.5	18.7
2	SD	2.3	33.8	41.5	32.2
1	SD	1.1	7.8	8.1	8.0
2	PR	5.2	38.1	44.3	39.4
3	SD	0.5	3.3	3.4	3.4
4	SD	2.1	15.6	16.0	15.8
1	PD	4.9	32.1	49.1	33.3
2	PD	10.8	71.6	73.5	53.9
3	PD	1.7	11.1	12.4	11.8
4	PD	2.3	14.9	19.1	17.4

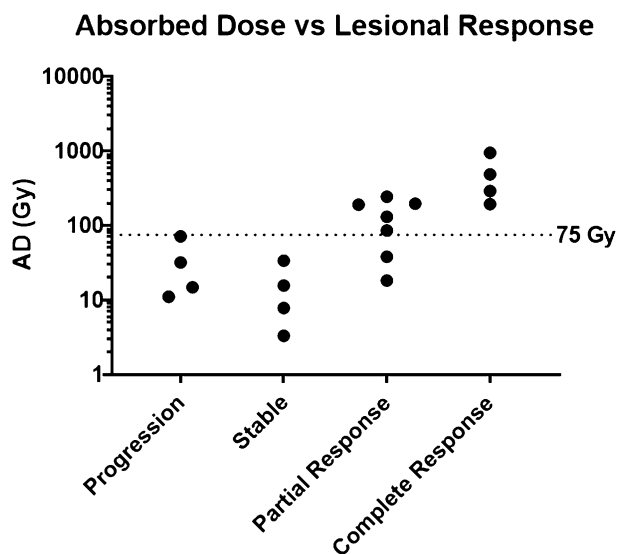


**Fig. 3** Absorbed dose versus lesion response

and equivalent uniform dose delivered from dosimetrically guided administered therapeutic activity of <sup>131</sup>I therapy with the lesional dosimetry performed based on <sup>124</sup>I PET/CT imaging. Jentzen et al. [14] reported absorbed dose versus clinical response in 59 lesions in 17 patients. However, the metric for their clinical response was whether or not the lesion was detectable on follow-up <sup>124</sup>I or <sup>131</sup>I diagnostic scans, and they acknowledged that this had a potentially significant limitation of failing to image a lesion that may still be present when its uptake is simply below the detection of the PET scanner. Wierts et al. [14] evaluated absorbed dose response in 47 patients using <sup>124</sup>I PET/CT dosimetry; however, their clinical response criteria were also whether or

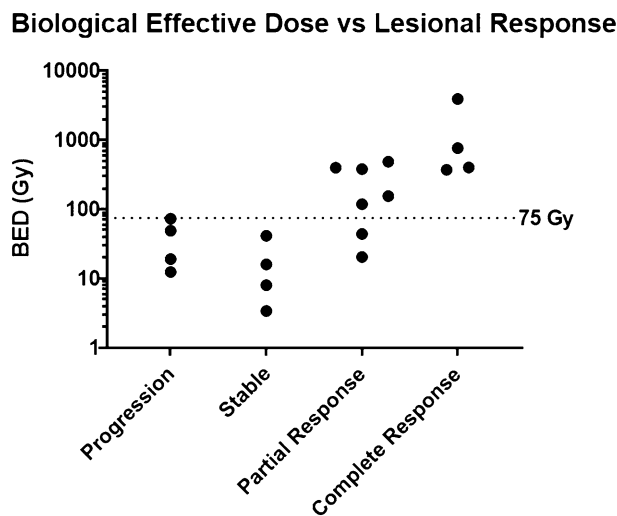


**Fig. 4** Biologically effective dose versus lesion response

### Equivalent Uniform Dose vs Lesional Response

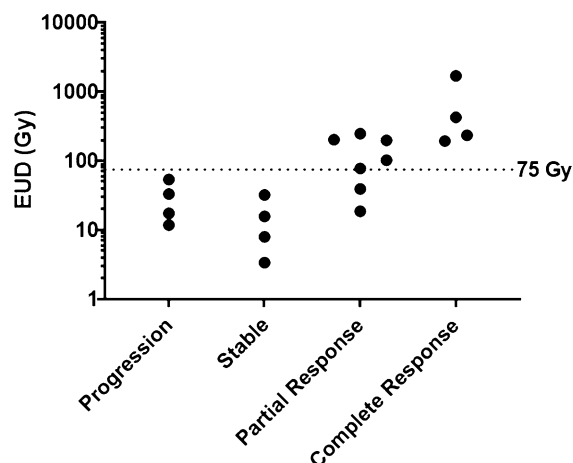


**Fig. 5** Equivalent uniform dose versus lesion response

not the lesion was detectable on follow-up  $^{124}\text{I}$  or  $^{131}\text{I}$  diagnostic images. In addition, the patients only received empiric therapeutic administered activities of  $3.0 \pm 1.0$  GBq. Hobbs et al. [11] compared  $^{124}\text{I}$  PET-based dosimetry to clinical outcomes based on  $^{124}\text{I}$  PET/CT imaging, but this was only performed in one pediatric patient.

Second, we evaluated not just one, but three dosimetric quantities (i.e., absorbed dose, biological effective dose, and equivalent uniform dose). Tumor response to dose depends on a variety of different factors and parameters, including dose rate and heterogeneity of dose, which are not accounted for in an absorbed dose fraction method which only provides the mean absorbed dose [36]. The BED is the dosimetric quantity that accounts for dose rate and; normal organ tissue responses have been shown to correlate better with BED than absorbed dose [37, 38]. A biological quantity such as the BED that incorporates dose rate effects in tumors will likely provide better correlation than the absorbed dose. The EUD represents a single dose value for a non-uniform BED distribution in a region or organ.

Third, we used a methodology for activity quantification in small volumes. The availability of patient-specific  $^{124}\text{I}$  PET/CT imaging data provided a framework for performing quantitative tumor activity measurements, which is essential for the accuracy of the dosimetric calculations. This, combined with the activity quantification method, potentially improves the accuracy of the absorbed dose calculations. In turn, the tumor AD and dose-rate values derived from the lesion activity measurements are directly related to the accuracy of BED and EUD calculations.

Finally, this study helps further establish a stronger relationship of absorbed dose to clinical response that is needed for the clinical implementation of patient-specific

pre-treatment planning for  $^{131}\text{I}$  therapy for DTC [11–14, 39]. It has been shown previously that retrospective dosimetry calculations can help establish dose–response relationships [11–14, 39]. Dewaraja et al. [11] demonstrated the importance of 3D calculation and radiobiologic modeling when estimating absorbed dose to predict patient outcome in patients receiving  $^{131}\text{I}$ -tositumomab for the treatment of refractory B cell lymphoma. Maxon et al. suggested that initial  $^{131}\text{I}$  treatments resulting in absorbed doses of at least 300 Gy (30,000 rad) to thyroid remnants and 80 Gy (8000 rad) to metastases were associated with a significant increase in the rate of response to therapy. In a study with 85 patients, Maxon et al. [40] reported that a uniformly good response should be possible if a minimal tumor dose of 8000 to 10,000 cGy (rad) could be achieved. Jentzen et al. [13] performed a retrospective analysis of the  $^{124}\text{I}$  imaging data to assess the therapy response above the accepted AD thresholds and to explore the relationship between therapy response and minimal lesional AD. For lesions  $>0.8$  ml, the response rate for thyroid remnants matched well with historical data derived using  $^{131}\text{I}$  scintigraphy imaging, whereas the response rate for lymph node metastases was not as high as expected [13]. Wierts et al. [14] found a statistically significant dose–response relationship for both thyroid remnants and metastases using pre-therapeutic  $^{124}\text{I}$  PET/CT lesion dosimetry. Except for the small lesions ( $<0.15$  ml), the lesional AD of completely responding lesions was significantly higher than that of incompletely responding lesions [14]. The corresponding lesional AD threshold value maximizing correct complete response prediction was 90 Gy for remnants and 40 Gy for metastases [14]. Hobbs et al. [10] demonstrated a real-time treatment planning using 3D RD using sequential  $^{124}\text{I}$  PET/CT imaging and providing more detailed information regarding potential efficacy and toxicity, underlining the importance of performing patient-specific radiobiological dosimetry to establish correlations between dosimetric quantities and patient’s response to therapy. In our study, 82% (9/11) of the CR and PR lesions had an absorbed dose of  $>75$  Gy (8000 rad), Fig. 3. All progressive and stable lesions received  $<75$  Gy. We submit—and as one would expect—that there is a greater probability that a DTC lesion will respond when the absorbed dose as well as the biological effective and equivalent uniform doses delivered to the lesion are higher.

This study has multiple limitations including a small number of patients, a modest number of target lesions, the use of modified RECIST criteria to evaluate response, and the quality of the available clinical response based on imaging and history. Other limitations include the non-availability of the status of the lesions prior to therapy, albeit the fact that the patient was referred for  $^{131}\text{I}$  therapy implies that some, if not all lesions, were progressing. Another limitation is that this study did not correlate untoward effects to



absorbed dose delivered to normal organs. Finally, limitations on absorbed dose calculations include the large uncertainties in volume of interest delineation that may directly propagate to the uncertainties in measuring the tumor activity in small volumes (i.e. < 10 ml [41]), and the accuracy of the activity measurement is directly related to the accuracy of the absorbed dose and other quantities, such as BED and EUD. The lesion size and the accuracy of activity measurement are especially important in the EUD calculation and its utility as a dosimetric quantity for correlating dosimetry in radiopharmaceutical therapy with treatment response. More specifically, activity is not accurately quantified at the voxel level, an admission exemplified by the methodology used to quantify the tumor activities. The consequences are that the tumor activity was assumed to be uniform and consequently that the EUD only accounted for edge-effect non-uniformities of BED and could not include any non-uniformity of activity effects.

Further studies are needed to determine and help establish a minimum AD, BED, and/or EUD value that must be delivered to various DTC distant metastases from a single therapeutic administration of  $^{131}\text{I}$  to achieve complete or partial response.

This study further cautions practicing physicians in assuming that “less is more”. In other words, one should not assume that by administering less therapeutic administered activity of  $^{131}\text{I}$  with the admirable intent of reducing side effects one will maintain equal clinical effectiveness. “Less-is-more” administered  $^{131}\text{I}$  activity only applies when the administered activity is still delivering a minimum therapeutic absorbed dose such as at least 80 Gy (8000 rad) to a metastasis. When one is reducing the administered empiric activity of  $^{131}\text{I}$ , such as to 3.7 GBq (100 mCi) and even as low as 1.1 GBq (30 mCi), there is an ever-increasing likelihood that the absorbed dose delivered will not be therapeutic. When the absorbed dose delivered is less than 80 Gy (8000 rad), there may indeed be less side effects but with reduced clinical effectiveness. In addition, the practicing physician should not conclude de facto that a lack of response, such as to activities of 5.5 GBq (150 mCi) or even 7.4 GBq (200 mCi) of  $^{131}\text{I}$ , is indicative of radioiodine refractory disease [42]. Rather, the lack of response may be a result of insufficient administered  $^{131}\text{I}$  activity.

To conclude, this study emphasizes the necessity of patient-specific dosimetry as predictor of therapeutic response in patients with metastatic DTC prior to treatment with  $^{131}\text{I}$ . To be administering empiric activities of  $^{131}\text{I}$  of 3.7 GB (100 mCi), 5.55 GBq (150 mCi), 7.4 GBq (200 mCi) or even more may not only be insufficient, but a waste of resources and money while achieving nothing but increased side effects. We should change our mantra for determining administered activity of  $^{131}\text{I}$  for treatment of DTC metastases from “less-is-more-empiric-activities” to

“patient-specific-dosimetrically guided activities” and preferably to “lesion-specific and organ-specific dosimetrically guided activities.”

## Summary

This study correlated lesion-specific clinical response of differentiated thyroid cancer metastases to absorbed dose delivered to the specific metastases with the absorbed dose based on (1) the patient’s therapeutic administered activity of  $^{131}\text{I}$ , (2) five-point  $^{124}\text{I}$  PET/CT scans and quantitation, (3) radiobiological dosimetric quantities of BED, and EUD in addition to absorbed dose calculations, and (4) an activity quantification method for small volumes/lesions.

For 82% (9/11) of lesions with complete remission or partial response, the calculated AD, BED and EUD values were greater than 75 Gy. The AD, BED, and EUD values for the stable and progressive disease lesions were less than 75 Gy.

**Funding** This project was supported in part by The Catherine Heron and Al Schneider Fellowship in Thyroid Cancer. Also, we would like to thank the support of donations from our grateful patients at MedStar Washington Hospital Center.

**Availability of Data and/or Code Availability** Data and code data are available upon request from the authors.

## Declarations

**Conflict of interest** Douglas Van Nostrand: speaker and consultant for Jubilant DraxImage. No competing financial interests exist for the remaining authors.

**Ethical approval** The original prospective study forming the source of this analysis of the data presented herein as well as this study itself were approved by the MedStar Health Institutional Review Board.

## References

1. Haugen BR, Alexander EK, Bible KC, Doherty GM, Mandel SJ, Nikiforov YE, et al. 2015 American Thyroid Association management guidelines for adult patients with thyroid nodules and differentiated thyroid cancer: the American Thyroid Association guidelines task force on thyroid nodules and differentiated thyroid cancer. *Thyroid*. 2016;26(1):1–133.
2. Van Nostrand D, Atkins F, Yeganeh F, Acio E, Bursaw R, Wartofsky L. Dosimetrically determined doses of radioiodine for the treatment of metastatic thyroid carcinoma. *Thyroid*. 2002;12(2):121–34.
3. Atkins F, Van Nostrand D, Wartofsky L. Dosimetrically determined prescribed activity of I-131 for the treatment of metastatic differentiated thyroid cancer. In: Wartofsky L, Van Nostrand D, editors. *Thyroid cancer: a comprehensive guide to clinical management*. Berlin: Springer; 2016. p. 635–50.

4. Benua RS, Cicale NR, Sonenberg M, Rawson R. The relation of radioiodine dosimetry to results and complications in the treatment of metastatic thyroid cancer. *Am J Roentgenol Radium Therapy Nucl Med.* 1962;87:171–82.
5. Dorn R, Kopp J, Vogt H, Heidenreich P, Carroll RG, Gulec SA. Dosimetry-guided radioactive iodine treatment in patients with metastatic differentiated thyroid cancer: largest safe dose using a risk-adapted approach. *J Nucl Med.* 2003;44(3):451–6.
6. Van Nostrand D, Atkins F, Moreau S, Aiken M, Kulkarni K, Wu JS, et al. Utility of the radioiodine whole-body retention at 48 hours for modifying empiric activity of <sup>131</sup>I-iodine for the treatment of metastatic well-differentiated thyroid carcinoma. *Thyroid.* 2009;19(10):1093–8.
7. Thomas SR, Maxon HR, Kereiakes JG. In vivo quantitation of lesion radioactivity using external counting methods. *Med Phys.* 1976;3(4):253–5.
8. Benua RS. A method and rationale for treating metastatic thyroid carcinoma with the largest safe dose of I-<sup>131</sup>. *Front Thyroidol.* 1986, pp. 1317–1321.
9. Lassmann M, Häscheid H, Verburg F, Luster M. The use of dosimetry in the treatment of differentiated thyroid cancer. *Q J Nucl Med Mol Imaging.* 2011;55(2):107–15.
10. Hobbs RF, Wahl RL, Lodge MA, Javadi MS, Cho SY, Chien DT, et al. <sup>124</sup>I PET-based 3D-RD dosimetry for a pediatric thyroid cancer patient: real-time treatment planning and methodologic comparison. *J Nucl Med.* 2009;50(11):1844–7.
11. Dewaraja YK, Schipper MJ, Roberson PL, Wilderman SJ, Amro H, Regan DD, et al. <sup>131</sup>I-tositumomab radioimmunotherapy: Initial tumor dose–response results using 3-dimensional dosimetry including radiobiologic modeling. *J Nucl Med.* 2010;51(7):1155–62.
12. Maxon HR, Thomas SR, Hertzberg VS, Kereiakes JG, Chen I-W, Sperling MI, et al. Relation between effective radiation dose and outcome of radioiodine therapy for thyroid cancer. *New Engl J Med.* 1983;309(16):937–41.
13. Jentzen W, Hoppenbrouwers J, van Leeuwen P, van der Velden D, van de Kolk R, Poeppel TD, et al. Assessment of lesion response in the initial radioiodine treatment of differentiated thyroid cancer using <sup>124</sup>I PET imaging. *J Nucl Med.* 2014;55(11):1759–65.
14. Wierths R, Brans B, Havekes B, Kemerink GJ, Halders SG, Schaper NN, et al. Dose–response relationship in differentiated thyroid cancer patients undergoing radioiodine treatment assessed by means of <sup>124</sup>I PET/CT. *J Nucl Med.* 2016;57(7):1027–32.
15. Cristy M, Eckerman K. Specific absorbed fractions of energy at various ages from internal photon sources: 1, methods. Oak Ridge: Oak Ridge National Lab; 1987.
16. Prideaux AR, Song H, Hobbs RF, He B, Frey EC, Ladenson PW, et al. Three-dimensional radiobiologic dosimetry: Application of radiobiologic modeling to patient-specific 3-dimensional imaging-based internal dosimetry. *J Nucl Med.* 2007;48(6):1008–16.
17. Plyku D, Hobbs RF, Huang K, Atkins F, Garcia C, Sgouros G, et al. Recombinant human thyroid-stimulating hormone versus thyroid hormone withdrawal in <sup>124</sup>I PET/CT-based dosimetry for <sup>131</sup>I therapy of metastatic differentiated thyroid cancer. *J Nucl Med.* 2017;58(7):1146–54.
18. Bolch WE, Eckerman KF, Sgouros G, Thomas SR. MIRD pamphlet no 21: a generalized schema for radiopharmaceutical dosimetry: standardization of nomenclature. *J Nucl Med.* 2009;50(3):477–84.
19. Plyku D, Lodge M, Van Nostrand D, Sgouros G, Hobbs R. Small volume activity quantification method for absorbed dose calculations. *J Nucl Med.* 2019;60(supplement 1):1135.
20. Hobbs R, Jentzen W, Bockisch A, Sgouros G. Monte Carlo-based 3-dimensional dosimetry of salivary glands in radioiodine treatment of differentiated thyroid cancer estimated using <sup>124</sup>I PET. *Q J Nucl Med Mol Imaging.* 2013;57(1):79.
21. Hobbs RF, Sgouros G. Calculation of the biological effective dose for piecewise defined dose-rate fits. *Med Phys.* 2009;36(3):904–7.
22. Hobbs RF, Wahl RL, Frey EC, Kasamon Y, Song H, Huang P, et al. Radiobiologic optimization of combination radiopharmaceutical therapy applied to myeloablative treatment of non-Hodgkin lymphoma. *J Nucl Med.* 2013;54(9):1535–42.
23. Dale RG. The application of the linear-quadratic dose-effect equation to fractionated and protracted radiotherapy. *B J Radiol.* 1985;58(690):515–28.
24. Baechler S, Hobbs RF, Prideaux AR, Wahl RL, Sgouros G. Extension of the biological effective dose to the MIRD schema and possible implications in radionuclide therapy dosimetry. *Med Phys.* 2008;35(3):1123–34.
25. Fowler JF. The linear-quadratic formula and progress in fractionated radiotherapy. *B J Radiol.* 1989;62(740):679–94.
26. Millar WT. Application of the linear-quadratic model with incomplete repair to radionuclide directed therapy. *Br J Radiol.* 1991;64(759):242–51.
27. Brenner DJ, Hlatky L, Hahnfeldt P, Huang Y, Sachs R. The linear-quadratic model and most other common radiobiological models result in similar predictions of time-dose relationships. *Radiat Res.* 1998;150(1):83–91.
28. Van Leeuwen C, Oei A, Crezee J, Bel A, Franken N, Stalpers L, et al. The alfa and beta of tumours: a review of parameters of the linear-quadratic model, derived from clinical radiotherapy studies. *Rad Oncol.* 2018;13(1):1–11.
29. Gaussen A, Legal J-D, Beron-Gaillard N, Laplanche A, Travagli J-P, Caillou B, et al. Radiosensitivity of human normal and tumoral thyroid cells using fluorescence in situ hybridization and clonogenic survival assay. *Int J Radiat Oncol Biol Phys.* 1999;44(3):683–91.
30. Challeton C, Branea F, Schlumberger M, Gaillard N, de Vathaire F, Badie C, et al. Characterization and radiosensitivity at high or low dose rate of four cell lines derived from human thyroid tumors. *Int J Radiat Oncol Biol Phys.* 1997;37(1):163–9.
31. Bodey R, Flux G, Evans P. Combining dosimetry for targeted radionuclide and external beam therapies using the biologically effective dose. *Cancer Biother Radiopharm.* 2003;18(1):89–97.
32. Sgouros G, Hobbs RF, Atkins FB, Van Nostrand D, Ladenson PW, Wahl RL. Three-dimensional radiobiological dosimetry (3D-RD) with <sup>124</sup>I PET for <sup>131</sup>I therapy of thyroid cancer. *Eur J Nucl Med Mol Imaging.* 2011;38(1):41–7.
33. Agostinelli S, Allison J, Ka A, Apostolakis J, Araujo H, Arce P, et al. GEANT4—a simulation toolkit. *Nucl Instrum Methods Phys Res Sect A.* 2003;506(3):250–303.
34. Chalian H, Töre HG, Horowitz JM, Salem R, Miller FH, Yaghmai V. Radiologic assessment of response to therapy: comparison of RECIST versions 1.1 and 1.0. *Radiographics.* 2011;31(7):2093–105.
35. Eisenhauer EA, Therasse P, Bogaerts J, Schwartz LH, Sargent D, Ford R, et al. New response evaluation criteria in solid tumours: revised RECIST guideline (version 1.1). *Eur J Cancer.* 2009;45(2):228–47.
36. Van Nostrand D, Hobbs R, Atkins FB, Sgouros G. <sup>124</sup>I in differentiated thyroid cancer. In: Wartofsky L, Van Nostrand D, editors. *Thyroid cancer: a comprehensive guide to clinical management.* Berlin: Springer; 2016. p. 973–89.
37. Freudenberg LS, Jentzen W, Petrich T, Frömke C, Marlowe RJ, Heusner T, et al. Lesion dose in differentiated thyroid carcinoma metastases after rhTSH or thyroid hormone withdrawal: <sup>124</sup>I PET/CT dosimetric comparisons. *Eur J Nucl Med Mol Imaging.* 2010;37(12):2267–76.
38. Khorjekar GR, Van Nostrand D, Garcia C, O’Neil J, Moreau S, Atkins FB, et al. Do negative <sup>124</sup>I pretherapy positron emission tomography scans in patients with elevated serum thyroglobulin

- levels predict negative <sup>131</sup>I posttherapy scans? *Thyroid*. 2014;24(9):1394–9.
39. Senthamizchelvan S, Hobbs RF, Song H, Frey EC, Zhang Z, Armour E, et al. Tumor dosimetry and response for <sup>153</sup>Sm-ethylenediamine tetramethylene phosphonic acid therapy of high-risk osteosarcoma. *J Nucl Med*. 2012;53(2):215–24.
40. Maxon HR 3rd, Englaro EE, Thomas SR, Hertzberg VS, Hinnefeld JD, Chen LS, Smith H, Cummings D, Aden MD. Radioiodine-131 therapy for well-differentiated thyroid cancer—a quantitative radiation dosimetric approach: outcome and validation in 85 patients. *J Nucl Med*. 1992;33(6):1132–6.
41. Gear JJ, Cox MG, Gustafsson J, Gleisner KS, Murray I, Glatting G, et al. EANM practical guidance on uncertainty analysis for molecular radiotherapy absorbed dose calculations. *Eur J Nucl Med Mol Imaging*. 2018;45(13):2456–74.
42. Van Nostrand D. Radioiodine refractory differentiated thyroid cancer: time to update the classifications. *Thyroid*. 2018;28(9):1083–93.

**Publisher's Note** Springer Nature remains neutral with regard to jurisdictional claims in published maps and institutional affiliations.